DOI: 10.1021/ma102275h

Macromolecules
ARTICLE

Low-Bandgap Conjugated Donor−Acceptor Copolymers Based on Porphyrin with Strong Two-Photon Absorption

Xuebin Huang,[†,‡] Qinqin Shi,[†,⊥] Wei-Qiang Chen,[§] Chunli Zhu,[†,‡] Weiyi Zhou,[†,⊥] Zhen Zhao,[†] Xuan-Ming Duan,*[,§] and Xiaowei Zhan*[,†]

[†]*Beijing National Laboratory for Molecular Sciences and Institute of Chemistry, Chinese Academy of Sciences, Beijing 100190, China,* [‡]*Department of Chemistry, Beijing Institute of Technology, Beijing 100083, China,* [§]*Laboratory of Organic Nanophotonics and Key Laboratory of Photochemical Convention and Functional Materials, Technical Institute of Physics and Chemistry, Chinese Academy of Sciences, Beijing 100190, China, and* [⊥]*Graduate University of Chinese Academy of Sciences, Beijing 100049, China*

Received October 4, 2010; Revised Manuscript Received November 3, 2010

ABSTRACT: Two new low-bandgap, conjugated donor (D)−acceptor (A) copolymers of porphyrin with 2,3-bis(4-trifluoromethylphenyl)pyrido[3,4-*b*]pyrazine (**P1**) and perylene diimide (**P2**) were synthesized by Sonogashira coupling polymerization and compared with porphyrin−dithienothiophene D−D copolymer (**P3**). All these polymers possess good thermal stability with decomposition temperatures over 300 °C. Polymers **P1** and **P2** in films exhibit strong absorption in near-IR (820−950 nm) with optical bandgaps as low as 1.15 eV; their Q-bands red shift 60−190 nm compared to that of **P3**, while the Soret bands are similar. The HOMO (−5.3 to −5.4 eV) and LUMO (−3.6 to −4.0 eV) of the D−A polymers are lower than that of the D−D polymer. Two-photon absorption (2PA) properties of the polymers were investigated by the femtosecond Z-scan method. The D−A polymer **P2** exhibits 2PA cross sections over 7000 GM/repeat unit at telecommunication wavelengths (1320 and 1520 nm), larger than that of **P1** and **P3**, due to the very strong, rigid, and coplanar perylene diimide acceptor and strong D−A intramolecular charge transfer.

Introduction

Conjugated polymers that have extended delocalized π-electron systems with their potential application in organic optoelectronic devices have been extensively investigated.[1−3] Recently, low-bandgap conjugated polymers have received considerable interest, specifically those with bandgaps below 1.5 eV.[4] These materials have unique electronic and optical properties including near-infrared (NIR) absorption, NIR emission, and solid-state charge transport.[5] These polymers can find applications in sensors, detectors, and telecommunication technologies.[6] Their strong visible and NIR absorption is beneficial to improve power conversion efficiency of polymer solar cells (PSCs). One way to design low-bandgap polymers is to alternate electron donor (D) and acceptor (A) units in the conjugated backbone of the polymers. The electronic structure (HOMO/LUMO levels and bandgap) of the polymers can be manipulated through the partial intramolecular charge transfer (ICT) along the main chains of the D−A systems.[7,8]

Materials with strong two-photon absorption (2PA) at telecommunication wavelengths (1.3 and 1.55 μm) are highly useful for signal processing such as optical power stabilization, pulse suppression, and optical limiting.[9,10] Compared with other chromophores such as dipolor,[11] singlet diradical,[12] and BODIPY dyes,[13] which exhibited 2PA cross sections (δ) below 1500 GM at these wavelengths, porphyrins, particularly with expanded or fused rings, exhibited larger δ up to 10^4 GM at telecommunication wavelengths due to their large and coplanar π-conjugated macrocycles, high transition dipole moments, and NIR absorption of Q bands.[14−19] The literature on porphyrin polymers with strong 2PA at telecommunication wavelengths is significantly sparser than that for their small molecule counterparts; there is only a single report of porphyrin polymers with strong 2PA at telecommunication wavelengths, wherein double-strand conjugated porphyrin ladder arrays exhibited δ of 8900 GM/repeat unit at 1325 nm.[20]

There have been several reports on D−A−D small molecules based on porphyrin.[21−23] It was experimentally and theoretically found that the intramolecular charge transfer between D and A units can induce 2PA enhancement.[24−27] However, to our knowledge, there have been no reports on D−A main-chain conjugated polymers based on porphyrin. We were interested in synthesis of π-conjugated D−A copolymers of porphyrin with perylene diimide (PDI) and pyridopyrazine based on the following considerations: (a) chromophores containing fused-ring units have conformational rigidity, which is a common feature of most leading 2PA materials; (b) fused-ring PDI[28−31] and fused-ring pyrazine[32−34] are strong π-electron acceptors (A), while porphyrin is a strong π-electron donor (D), and A, D, and a polarizable π-bridge are three essential components required for strong 2PA dyes. Here we report two new low-bandgap π-conjugated D−A copolymers of porphyrin with pyridopyrazine and PDI (**P1** and **P2**, Figure 1). They exhibit strong NIR absorption and large 2PA cross sections at telecommunication wavelengths (1.32 and 1.52 μm). We also compare these D−A copolymers with the porphyrin−dithienothiophene (D−D) copolymer[35] (**P3**, Figure 1) and investigate effect of the counits on the electronic and photonic properties of the polymers.

Results and Discussion

Synthesis and Characterization of the Polymers. Synthetic routes to the porphyrin polymers **P1** and **P2** are shown in Scheme 1. Polymer **P3**,[35] diethynylporphyrin (**1**),[35] and electron-withdrawing monomer 5,8-dibromo-2,3-bis(4-trifluoromethylphenyl)pyrido[3,4-*b*]pyrazine (**2**)[32] were synthesized

*Corresponding authors. E-mail: xwzhan@iccas.ac.cn.

 Published on Web 11/15/2010

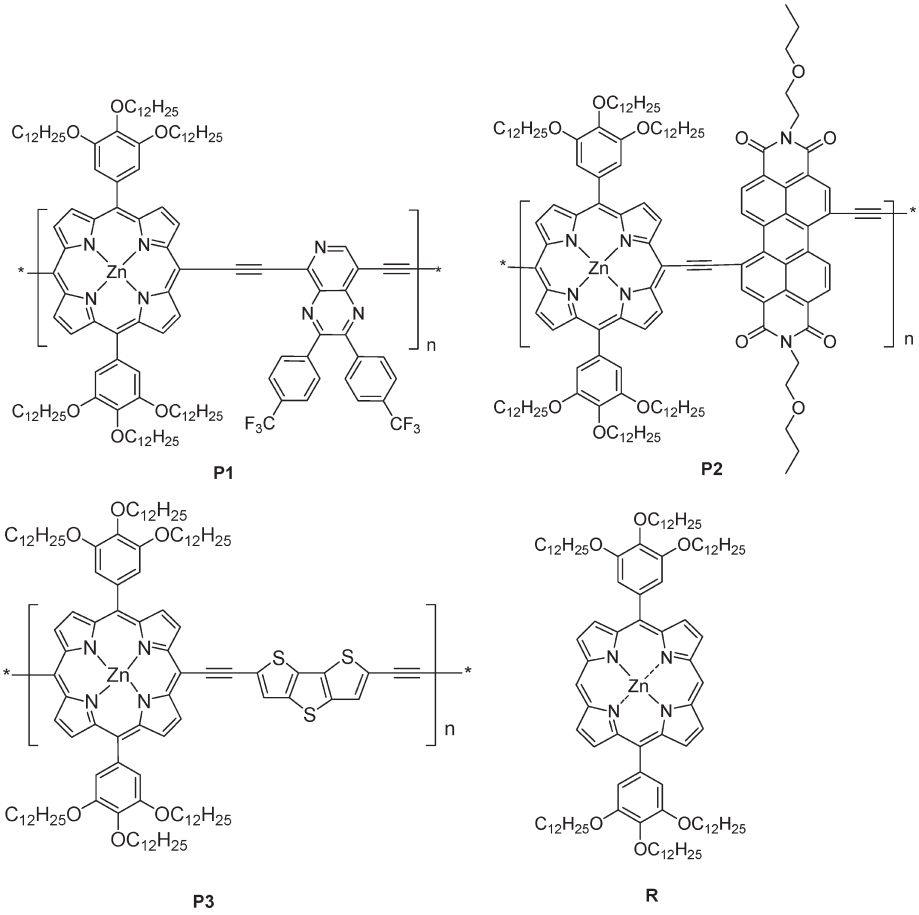

Figure 1. Chemical structures of porphyrin polymers and reference molecule.

according to our reported procedures. New electron-withdrawing monomer *N*,*N*′-bis(2-propoxyethyl)-1,7-dibromo-3,4:9,10-perylene diimide (**3**) was synthesized by condensation of 1,7-dibromoperylene dianhydride with the amine in 81% yield. Polymers **P1** and **P2** were synthesized through Sonogashira coupling reaction of diethynyl-substituted porphyrin (**1**) with dibromo-substituted pyrazine (**2**) and PDI (**3**) in high yields.

All these polymers are readily soluble in common organic solvents such as chloroform, THF, and toluene because of the solubilizing 3,4,5-tridodecyloxyphenyl groups at positions 10 and 20 of the zinc porphyrin ring of the polymers. Molecular weights of the polymers were determined by gel permeation chromatography (GPC) using polystyrene standards as calibrants (Table 1). The number-average molecular weights (M_n) of **P1**−**P3** were found to be 15 000−44 000 with polydispersity index (M_w/M_n) of 1.8−2.2. The thermal properties of the polymers were determined by thermogravimetric analysis (TGA) under nitrogen. All polymers have good thermal stability with decomposition temperatures (5% weight loss) over 300 °C (Figure 2).

Absorption Spectra. Figure 3a shows the UV−vis spectra of the porphyrin polymers and the porphyrin small molecule (**R**) in chloroform. The porphyrin small molecule (**R**) shows typical Soret and Q-band at 412 and 538 nm, respectively. Compared to that of the small molecule, the Soret band and Q-band of the polymers are broadened and red-shifted remarkably, especially the Q-band due to extended conjugation. In comparison with that for reference **R**, Q-band of the D−D polymer **P3** with dithienothiophene (DTT) counit shows a red shift of 167 nm, while Q-band of polymers **P1** and **P2**, which contain strong electron-withdrawing pyrazine and PDI counits, red shifts 298 and 374 nm, respectively. The significant further red shift of the Q-band of polymers **P1** and **P2** is attributed to the intramolecular charge transfer between the strong donor porphyrin and the strong acceptor pyrazine or PDI; the electron-withdrawing abilities of the electron acceptors play an important role in forming effective D−A intramolecular charge transfer.[36−39] The Soret band of D−A polymers **P1** and **P2** is insensitive to the solvent polarity, but their ICT band (Q-band) red shifts with increasing the solvent polarity. For example, the Q-band of **P2** red shifts 22 nm upon changing the solvent from chloroform to THF. The excited state of **P2** is stabilized by polar solvent, leading to red shift of absorption.[40]

The UV−vis absorption spectra of the polymers in thin film are shown in Figure 3b. The Soret bands of polymers **P1**−**P3** red shift compared to that in solution. The Q-band of **P1** blue shifts 16 nm, and its absorbance decreases relative to that in solution. The Q-band of **P2** and **P3** red shifts 36−56 nm and strengthens compared to that in solution, suggesting that these two compounds exhibit strong electronic coupling between neighboring molecules in films due to relatively large and coplanar structure of PDI and DTT counits. The D−A copolymers **P1** and **P2** exhibit strong absorption in NIR region (820−950 nm). The optical bandgaps of the D−A polymers, estimated from the absorption edge in films, are 1.38 and 1.15 eV for **P1** and **P2**, respectively, lower than that of the D−D polymer **P3** (Table 2).

Electrochemistry. Cyclic voltammetry (CV) was carried out under nitrogen on a deoxygenated solution of tetra-*n*-butylammonium hexafluorophosphate (0.1 M) in acetonitrile to investigate the electrochemical behavior of the polymers. Cyclic voltammograms of the D−A polymers

Scheme 1. Synthesis of the Porphyrin Polymers

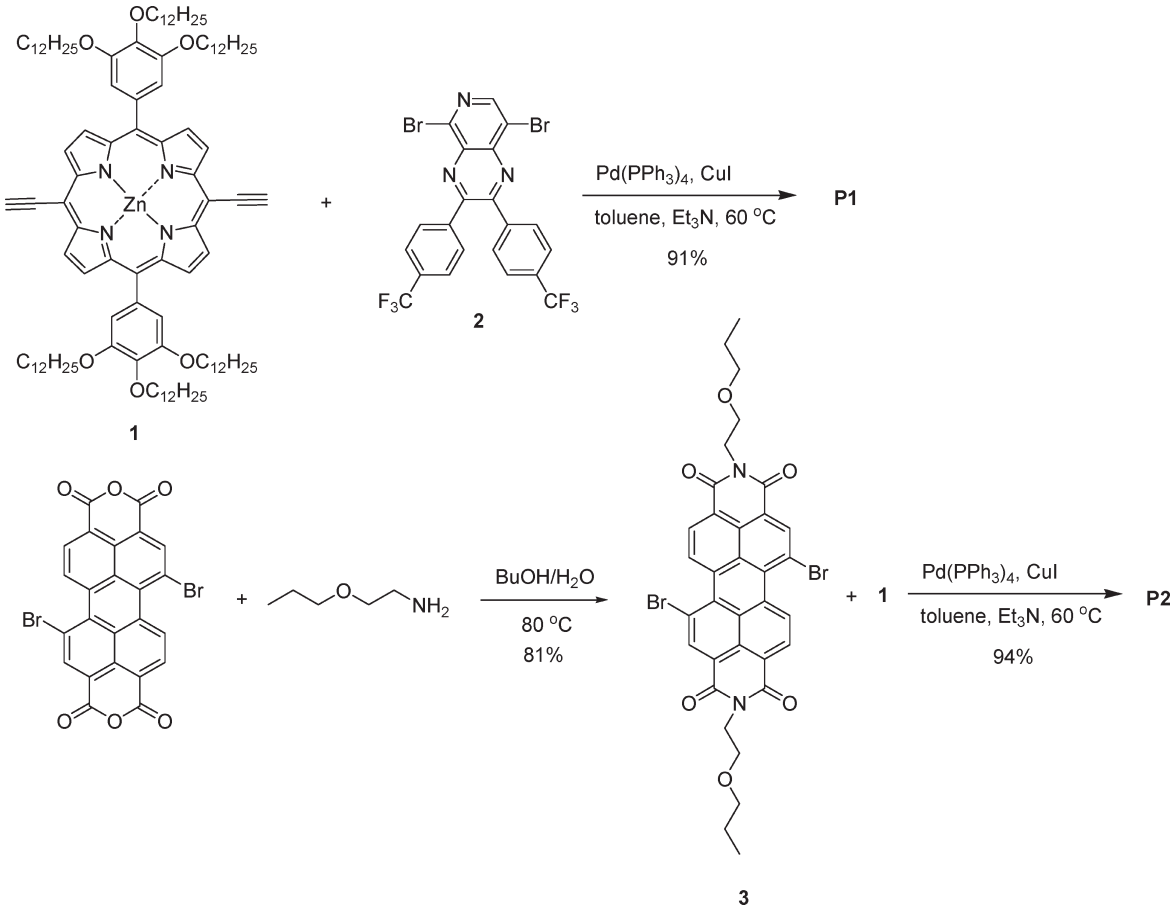

Table 1. Molecular Weights of the Polymers[a]

	M_n	M_w	M_w/M_n
P1	15 000	30 000	2.0
P2	44 000	98 000	2.2
P3	15 300	26 900	1.8

[a] Number-average molecular weight (M_n), weight-average molecular weight (M_w), and polydispersity index (M_w/M_n) determined by means of GPC with THF as eluent on the basis of polystyrene calibration.

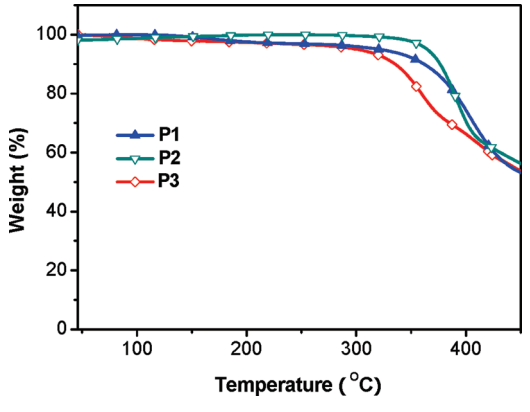

Figure 2. TGA curves of the polymers.

are illustrated in Figure 4. Polymer **P1** shows one irreversible oxidation peak and one quasi-reversible reduction peak, while polymer **P2** shows one reversible oxidation peak and one reversible reduction peak. The highest occupied molecular orbital (HOMO) and lowest unoccupied molecular orbital (LUMO) energy levels of the polymers were estimated from their onset oxidation potentials and onset reduction potentials, respectively (Table 3). The estimated HOMOs of the D−A polymers are ca. −5.3 to −5.4 eV, lower than that of the D−D polymer due to the electron-donating dithienothiophene unit in **P3**. The estimated LUMOs are sensitive to the counits. **P3** with a D−D structure has a LUMO of −3.24 eV, while **P1** and **P2** containing strong electron-withdrawing pyrazine and PDI counits exhibit lower LUMOs (−3.60 and −4.00 eV, respectively), which are similar to that of D−A copolymers based on pyrazine[33] and PDI,[28,41] suggesting that the LUMO wave function is localized on the acceptor units. As we expected, by increasing the electron-withdrawing strength of the counit, the HOMO−LUMO gap of the polymers decreases from 1.92 eV for **P3** to 1.71 eV for **P1** and 1.41 eV for **P2**. It means that we can modulate the LUMO and HOMO−LUMO gap of the D−A copolymers by changing the electron-withdrawing strength of the electron acceptors.

Two-Photon Absorption at Telecommunication Wavelengths. Two-photon absorption (2PA) is a way of accessing a given excited state by using photons of nearly half the energy (or nearly double the wavelength) of the corresponding one-photon transition. Since **P1**−**P3** in chloroform solution exhibit strong one-photon absorption at 700−900 nm, they may exhibit strong two-photon absorption at telecommunication wavelengths (1300−1500 nm). The 2PA cross sections δ of **P1**−**P3** were measured at 1320 and 1520 nm in $CHCl_3$ by using the open-aperture Z-scan method. Figure 5 shows typical Z-scan traces of **P1**−**P3** at 1320 and 1520 nm. The open-aperture traces exhibit a clear dip. The Z-scan traces of **P1**−**P3** at these two wavelengths clearly show a considerable dispersion and great 2PA effect. All polymers exhibit large

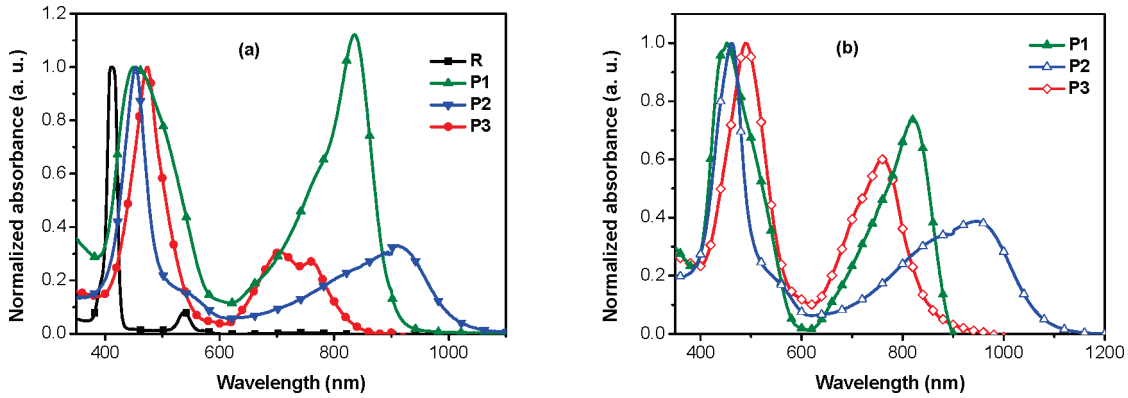

Figure 3. UV−vis absorption spectra of the porphyrin polymers as well as the reference molecule in chloroform (a) and in thin film (b).

Table 2. Absorption Maxima of the Polymers in $CHCl_3$ Solution and in Thin Film

	λ_{max} (nm) in solution		λ_{max} (nm) in film		
	Soret band	Q-band	Soret band	Q-band	E_g[a] (eV)
P1	450	836	452	820	1.38
P2	454	912	462	948	1.15
P3	474	705	489	761	1.47

[a] Optical bandgap estimated from the onset edge of absorption spectra in solid films.

2PA cross sections of 3000−8000 GM/repeat unit at both 1320 and 1520 nm (Table 4). Particularly, the D−A polymer **P2** exhibits δ over 7000 GM/repeat unit at both 1320 and 1520 nm, probably due to the very strong, rigid, and coplanar PDI acceptor. The δ value of **P2** is among the highest reported for organic 2PA dyes measured at telecommunication wavelengths.[11−20] Although the D−A polymer **P1** exhibits strong intramolecular charge transfer, it exhibits smaller δ relative to **P2** due to the rotational disorder of pyridopyrazine. On the other hand, although the D−D polymer **P3** has rigid and coplanar dithienothiophene unit, it exhibits smaller δ relative to **P2** due to lack of D−A intramolecular charge transfer. Therefore, D−A intramolecular charge transfer and rigid and coplanar structure play important roles in 2PA enhancement.

Conclusion

Two new low-bandgap, conjugated D−A copolymers of porphyrin donor with strong acceptors pyrido[3,4-*b*]pyrazine (**P1**) and PDI (**P2**) were synthesized by Sonogashira coupling polymerization. These polymers exhibit good solution processability, good thermal stability, and strong NIR absorption. Compared to the D−D polymer **P3** with electron-donating dithienothiophene unit, polymers **P1** and **P2** with strong acceptor units exhibit lower HOMO and LUMO levels, significantly red-shifted absorption spectra and lower bandgaps. The LUMOs and bandgaps of the polymers can be tuned by changing the electron-withdrawing ability of the acceptor unit. The D−A polymer **P2** exhibits 2PA cross sections over 7000 GM/repeat unit at both 1320 and 1520 nm, larger than that of **P1** and **P3**, due to the very strong, rigid, and coplanar PDI acceptor. The δ value of **P2** is among the highest reported for organic 2PA dyes measured at telecommunication wavelengths. The origins for large δ value of **P2** as follows: (a) Large, π-conjugated macrocycles, such as porphyrin and perylene diimide, are good candidates for two-photon dyes because of their high transition dipole moments. (b) Conformational rigidity and strong π conjugation of the backbone of the porphyrin and perylene diimide copolymer lead to the coherence of the wave function and the electron delocalization along the main chain. (c) From the viewpoint of electronic structures and photophysical processes, the intramolecular charge transfer between strong donor porphyrin and strong acceptor perylene diimide can induce 2PA enhancement.

Experimental Section

Materials. **P3**,[35] 5,15-diethynyl-10,20-bis(3,4,5-tridodecyloxyphenyl)porphyrinatozinc(II) (**1**),[35] and 5,8-dibromo-2,3-bis(4-trifluoromethylphenyl)pyrido[3,4-*b*]pyrazine (**2**)[32] were synthesized according to our published methods. Toluene was distilled from sodium benzophenone under nitrogen prior to use. Triethylamine was distilled from CaH_2 under nitrogen prior to use. All other reagents were used as received.

Characterization. The ^1H and ^{13}C NMR spectra were measured on a Bruker AVANCE 400 MHz spectrometer using tetramethylsilane (TMS; δ = 0 ppm) as an internal standard. Mass spectra were measured on a GCT-MS micromass spectrometer using the electron impact (EI) mode or on a Bruker Daltonics BIFLEX III MALDI-TOF analyzer using MALDI mode. Elemental analyses were carried out using a FLASH EA1112 elemental analyzer. Solution (chloroform) and thin-film (on quartz substrate) UV−vis absorption spectra were recorded on a JASCO V-570 spectrophotometer. Electrochemical measurements were carried out under nitrogen on a deoxygenated solution of tetra-*n*-butylammonium hexafluorophosphate (0.1 M) in acetonitrile using a computer-controlled Zahner IM6e electrochemical workstation, a glassy-carbon working electrode coated with polymer films, a platinum-wire auxiliary electrode, and an Ag wire anodized with AgCl as a pseudoreference electrode. Potentials were referenced to the ferrocenium/ferrocene ($FeCp_2^{+/0}$) couple by using ferrocene as an internal standard. Thermogravimetric analysis (TGA) measurements were performed on Shimadzu thermogravimetric analyzer (model DTG-60) under a nitrogen flow at a heating rate of 10 °C/min. The gel permeation chromatography (GPC) measurements were performed on a Waters 515 chromatograph connected to a Waters 2414 refractive index detector, using THF as eluent and polystyrene standards as calibrants. Three Waters Styragel columns (HT2, 3, 4) connected in series were used.

2PA Measurement. The 2PA cross sections δ of **P1**−**P3** were measured at 1320 and 1520 nm in $CHCl_3$ by using the open-aperture Z-scan method,[42,43] with ~120 fs pulses from an optical parametric amplify (OPA) operating at a 1 kHz repetition rate generated from a mode-locked Ti: sapphire femtosecond laser (Tsunami, Spectra-Physics). The laser beam was divided into two parts. One was used as the intensity reference and monitored by EPM 2000 power meter (Coherent Inc.). The other was used for transmittance measurement; the laser beam was focused by passing through len (f = 15 cm) and passed through a quartz cell with a sample thickness of 1 mm. The position of the sample cell could be varied along the laser-beam direction (z-axis), so the local power density within the sample cell could

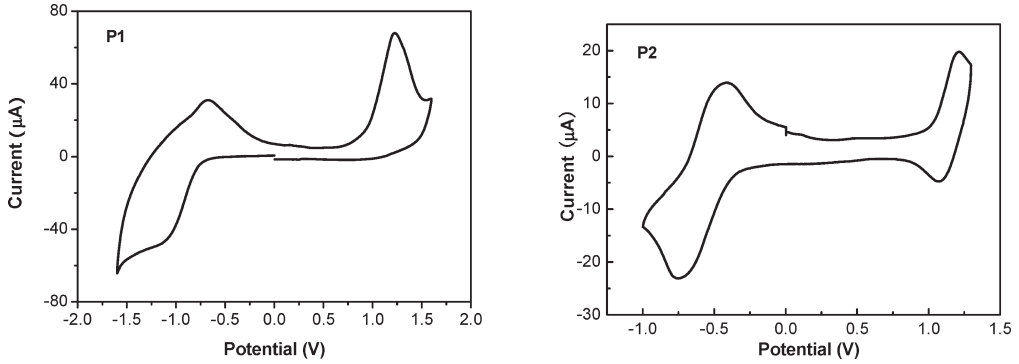

Figure 4. Cyclic voltammograms for the polymers in CH_3CN/0.1 M $[^nBu_4N]^+[PF_6]^-$ at 50 mV/s. The horizontal scale refers to an anodized Ag wire pseudoreference electrode.

Table 3. Redox Potentials and Energy Levels of the Polymers[a]

	E_{ox}[b] (V)	E_{red}[b] (V)	HOMO[c] (eV)	LUMO[c] (eV)	E_g[d] (eV)
P1	0.51	−1.20	−5.31	−3.60	1.71
P2	0.61	−0.80	−5.41	−4.00	1.41
P3	0.36	−1.56	−5.16	−3.24	1.92

[a] Thin films in CH_3CN/0.1 M $[^nBu_4N]^+[PF_6]^-$, versus ferrocenium/ferrocene at 50 mV s^{-1}. [b] E_{ox} is the onset potentials corresponding to oxidations, while E_{red} is the onset potentials corresponding to reductions. [c] HOMO and LUMO estimated from the onset oxidation and reduction potentials, respectively, assuming the absolute energy level of ferrocene/ferrocenium to be 4.8 eV below vacuum. [d] HOMO−LUMO gap obtained from electrochemistry.

be changed under a constant laser power level. The transmitted laser beam from the sample cell was then detected by the same power meter as used for reference monitoring. The on-axis peak intensity of the incident pulses at the focal point, I_0, ranged from 40 to 65 GW/cm^2. Assuming a Gaussian beam profile, the nonlinear absorption coefficient β can be obtained by curve fitting to the observed open-aperture traces with eq 1.

$$T(z) = 1 - \frac{\beta I_0 (1 - e^{-\alpha_0 l})}{2\alpha_0 (1 + (z/z_0)^2)} \quad (1)$$

where α_0 is the linear absorption coefficient, l the sample length, and z_0 the diffraction length of the incident beam. We obtained the nonlinear absorption coefficient β at the corresponding wavelength, where linear absorption is negligible, to satisfy the condition of $\alpha_0 l \ll 1$. When $\alpha_0 l \ll 1$, eq 1 can be simplified as eq 2.

$$T(z) = 1 - \frac{\beta I_0 l}{2(1 + (z/z_0)^2)} \quad (2)$$

The 2PA cross-section δ/repeated unit of **P1**−**P3** (in units of 1 GM = 1 × 10^{-50} cm^4/s) can be determined by eq 3.

$$\beta = \frac{\delta N_A d \times 10^{-3}}{h\nu} \quad (3)$$

where N_A is the Avogadro constant, d is the concentration of the repeated unit of **P1**−**P3** in $CHCl_3$ (the corresponding concentrations for **P1**−**P3** are 1.62 × 10^{-4}, 0.98 × 10^{-4}, and 1.28 × 10^{-4} M, respectively), h is the Planck constant, and ν is the frequency of the incident laser beam.

***N,N*-Bis(2-propoxyethyl)-1,7-dibromo-3,4:9,10-perylene Diimide (3).** 1,7-Dibromoperylene-3,4:9,10-tetracarboxylic acid dianhydride (275 mg, 0.5 mmol) in 20 mL of $^nBuOH/H_2O$ (1:1, v/v) was sonicated for 10 min. 2-Propoxyethanamine (180 mg, 1.75 mmol) was added, and the reaction mixture was stirred at 80 °C for 24 h under nitrogen. Concentrated aqueous HCl (2 mL) was added, and the mixture was stirred at room temperature for 30 min. The mixture was extracted with chloroform (2 × 25 mL), washed

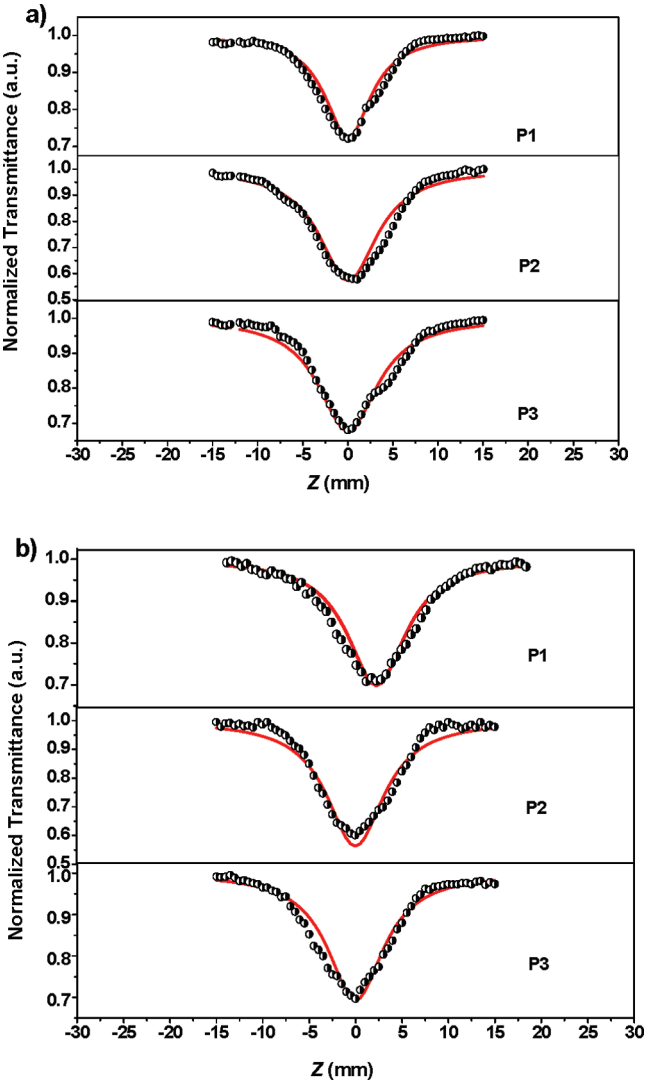

Figure 5. Z-scan trace (circle) of **P1**−**P3** in $CHCl_3$ in a 1 mm cell at (a) 1320 nm (I_0 = 62.6 GW/cm^2) and (b) 1520 nm (I_0 = 47.2 GW/cm^2) with a theoretical fit assuming a 2PA process (solid line).

Table 4. 2PA Cross Sections per Repeat Unit at Telecommunication Wavelengths for P1−P3

	δ (GM) at 1320 nm	δ (GM) at 1520 nm
P1	3220	3230
P2	7041	7704
P3	4067	4149

with water (2 × 300 mL), and dried over anhydrous $MgSO_4$. The solvent was removed and the residue was purified by column chromatography over silica gel eluting with $CHCl_3$/hexane (1:1) to give a red solid (290 mg, 81%). ^{1}H NMR (400 MHz, $CDCl_3$): δ 9.41 (d, J = 8.1 Hz, 2H), 8.86 (s, 2H), 8.64 (d, J = 8.2 Hz, 2H), 4.46 (t, J = 6.0 Hz, 4H), 3.78 (t, J = 5.9 Hz, 4H), 3.47 (t, J = 6.3 Hz, 4H), 1.55 (m, 4H), 0.87 (t, J = 7.4 Hz, 6H). ^{13}C NMR (100 MHz, $CDCl_3$): δ 163.09, 162.23, 136.77, 132.48, 131.00, 130.02, 128.88, 127.21, 126.85, 123.00, 122.51, 120.78, 72.69, 67.87, 39.66, 22.83, 11.32. MS (MALDI): 720 (M^+). Anal. Calcd for $C_{34}H_{28}Br_2N_2O_6$: C, 56.69; H, 3.92; N, 3.89. Found: C, 56.58; H, 3.93; N, 4.07%.

Poly{[5,15-diethynyl-10,20-bis(3,4,5-tridodecyloxyphenyl)porphyrinatozinc(II)]-*alt*-[2,3-bis(4-trifluoromethylphenyl)pyrido-[3,4-*b*]pyrazine-5,8-diyl]} (P1). To a 50 mL round-bottom flask were added 5,15-diethynyl-10,20-bis(3,4,5-tridodecyloxyphenyl)-porphyrinatozinc(II) (**1**) (336 mg, 0.2 mmol), 5,8-dibromo-2,3-bis(4-trifluoromethylphenyl)pyrido[3,4-*b*]pyrazine (**2**) (115 mg, 0.2 mmol), anhydrous toluene (10 mL), and triethylamine (5 mL). The mixture was deoxygenated with nitrogen for 30 min. $Pd(PPh_3)_4$ (23 mg, 0.02 mmol) and CuI (8 mg, 0.04 mmol) were added under nitrogen. The mixture was stirred at room temperature for 1 day and at 60 °C for 2 days. After being cooled to room temperature, the reaction mixture was added chloroform (50 mL) and filtered. The solution was concentrated and dropped into methanol (100 mL). After filtration, the polymer was purified by size exclusion column chromatography over Bio-Rad Bio-Beads S-X1 eluting with THF to afford a black solid (380 mg, 91%). ^{1}H NMR (400 MHz, $CDCl_3$): δ 10.1 (br, 1H), 9.0 (br, 8H), 7.8 (br, 8H), 7.0 (br, 4H), 4.6−4.0 (br, 12H), 2.2−0.7 (br, 138H). Anal. Calcd for $(C_{129}H_{171}F_6N_7O_6Zn)_n$: C, 73.95; H, 8.23; N, 4.68. Found: C, 70.81; H, 7.91; N, 4.30%. M_w 30 000; M_w/M_n, 2.0.

Poly{[5,15-diethynyl-10,20-bis(3,4,5-tridodecyloxyphenyl)-porphyrinatozinc(II)]-*alt*-[*N*,*N*′-bis(2-propoxyethyl)-3,4:9,10-perylene diimide-1,7-diyl]} (P2). To a 50 mL round-bottom flask were added 5,15-diethynyl-10,20-bis(3,4,5-tridodecyloxyphenyl)-porphyrinatozinc(II) (**1**) (168 mg, 0.1 mmol), *N*,*N*′-bis(2-propoxyethyl)-1,7-dibromo-3,4:9,10-perylene diimide (**3**) (72 mg, 0.1 mmol), anhydrous toluene (6 mL), and triethylamine (3 mL). The mixture was deoxygenated with N_2 for 30 min. $Pd(PPh_3)_4$ (12 mg, 0.01 mmol) and CuI (4 mg, 0.02 mmol) were added under nitrogen. The mixture was stirred at room temperature for 1 day and at 60 °C for 2 days. After being cooled to room temperature, the reaction mixture was added chloroform (10 mL) and filtered. The solution was concentrated and dropped into methanol (100 mL). After filtration, the polymer was purified by size exclusion column chromatography over Bio-Rad Bio-Beads S-X1 eluting with THF to afford a black solid (210 mg, 94%). ^{1}H NMR (400 MHz, $CDCl_3$): δ 10.0−8.0 (br, 14H), 7.0 (br, 4H), 4.8−3.5 (br, 24H), 2.4−0.7 (br, 148H). Anal. Calcd for $(C_{142}H_{190}N_6O_{12}Zn)_n$: C, 76.19; H, 8.56; N, 3.75. Found: C, 72.56; H, 8.22; N, 3.60%. M_w 98 000; M_w/M_n 2.2.

Acknowledgment. This work was supported by the NSFC (Grants 20774104, 21025418, 20702004, and 50973011) and the Chinese Academy of Sciences.

References and Notes

(1) Chen, L. M.; Hong, Z. R.; Li, G.; Yang, Y. *Adv. Mater.* **2009**, *21*, 1434.
(2) Hoven, C. V.; Garcia, A.; Bazan, G. C.; Nguyen, T. Q. *Adv. Mater.* **2008**, *20*, 3793.
(3) Fischer, M. K. R.; Kaiser, T. E.; Wurthner, F.; Bauerle, P. *J. Mater. Chem.* **2009**, *19*, 1129.
(4) Walker, W.; Veldman, B.; Chiechi, R.; Patil, S.; Bendikov, M.; Wudl, F. *Macromolecules* **2008**, *41*, 7278.
(5) Steckler, T. T.; Zhang, X.; Hwang, J.; Honeyager, R.; Ohira, S.; Zhang, X. H.; Grant, A.; Ellinger, S.; Odom, S. A.; Sweat, D.; Tanner, D. B.; Rinzler, A. G.; Barlow, S.; Bredas, J. L.; Kippelen, B.; Marder, S. R.; Reynolds, J. R. *J. Am. Chem. Soc.* **2009**, *131*, 2824.
(6) Chen, M. X.; Crispin, X.; Perzon, E.; Andersson, M. R.; Pullerits, T.; Andersson, M.; Inganas, O.; Berggren, M. *Appl. Phys. Lett.* **2005**, *87*, 252105.
(7) Bredas, J. L. *J. Chem. Phys.* **1985**, *82*, 3808.
(8) Roncali, J. *Chem. Rev.* **1997**, *97*, 173.
(9) Zheng, Q. D.; He, G. S.; Prasad, P. N. *Chem. Phys. Lett.* **2009**, *475*, 250.
(10) Bouit, P. A.; Wetzel, G.; Berginc, G.; Loiseaux, B.; Toupet, L.; Feneyrou, P.; Bretonniere, Y.; Kamada, K.; Maury, O.; Andraud, C. *Chem. Mater.* **2007**, *19*, 5325.
(11) Beverina, L.; Fu, J.; Leclercq, A.; Zojer, E.; Pacher, P.; Barlow, S.; Van Stryland, E. W.; Hagan, D. J.; Brédas, J. L.; Marder, S. R. *J. Am. Chem. Soc.* **2005**, *127*, 7282.
(12) Kamada, K.; Ohta, K.; Kubo, T.; Shimizu, A.; Morita, Y.; Nakasuji, K.; Kishi, R.; Ohta, S.; Furukawa, S.; Takahashi, H.; Nakano, M. *Angew. Chem., Int. Ed.* **2007**, *46*, 3544.
(13) Bouit, P. A.; Kamada, K.; Feneyrou, P.; Berginc, G.; Toupet, L.; Maury, O.; Androud, C. *Adv. Mater.* **2009**, *21*, 1151.
(14) Pawlicki, M.; Collins, H. A.; Denning, R. G.; Anderson, H. L. *Angew. Chem., Int. Ed.* **2009**, *48*, 3244.
(15) Tanaka, Y.; Saito, S.; Mori, S.; Aratani, N.; Shinokubo, H.; Shibata, N.; Higuchi, Y.; Yoon, Z. S.; Kim, K. S.; Noh, S. B.; Park, J. K.; Kim, D.; Osuka, A. *Angew. Chem., Int. Ed.* **2008**, *47*, 681.
(16) Yoon, M. C.; Noh, S. B.; Tsuda, A.; Nakamura, Y.; Osuka, A.; Kim, D. *J. Am. Chem. Soc.* **2007**, *129*, 10080.
(17) Inokuma, Y.; Ono, N.; Uno, H.; Kim, D. Y.; Noh, S. B.; Kim, D.; Osuka, A. *Chem. Commun.* **2005**, 3782.
(18) Mori, S.; Kim, K. S.; Yoon, Z. S.; Noh, S. B.; Kim, D.; Osuka, A. *J. Am. Chem. Soc.* **2007**, *129*, 11344.
(19) Kurotobi, K.; Kim, K. S.; Noh, S. B.; Kim, D.; Osuka, A. *Angew. Chem., Int. Ed.* **2006**, *45*, 3944.
(20) Drobizhev, M.; Stepanenko, Y.; Rebane, A.; Wilson, C. J.; Screen, T. E. O.; Anderson, H. L. *J. Am. Chem. Soc.* **2006**, *128*, 12432.
(21) Kelley, R. F.; Shin, W. S.; Rybtchinski, B.; Sinks, L. E.; Wasielewski, M. R. *J. Am. Chem. Soc.* **2007**, *129*, 3173.
(22) Susumu, K.; Duncan, T. V.; Therien, M. J. *J. Am. Chem. Soc.* **2005**, *127*, 5186.
(23) Odom, S. A.; Webster, S.; Padilha, L. A.; Peceli, D.; Hu, H.; Nootz, G.; Chung, S.-J.; Ohira, S.; Matichak, J. D.; Przhonska, O. V.; Kachkovski, A. D.; Barlow, S.; Brédas, J.-L.; Anderson, H. L.; Hagan, D. J.; Van Stryland, E. W.; Marder, S. R. *J. Am. Chem. Soc.* **2009**, *131*, 7510.
(24) Kim, K. S.; Noh, S. B.; Katsuda, T.; Ito, S.; Osuka, A.; Kim, D. *Chem. Commun.* **2007**, 2479.
(25) Humphrey, J. L.; Kuciauskas, D. *J. Am. Chem. Soc.* **2006**, *128*, 3902.
(26) Luo, Y.; Rubio-Pons, O.; Guo, J. D.; Agren, H. *J. Chem. Phys.* **2005**, *122*, 096101.
(27) Rubio-Pons, O.; Luo, Y.; Agren, H. *J. Chem. Phys.* **2006**, *124*, 094310.
(28) Zhan, X. W.; Tan, Z. A.; Domercq, B.; An, Z. S.; Zhang, X.; Barlow, S.; Li, Y. F.; Zhu, D. B.; Kippelen, B.; Marder, S. R. *J. Am. Chem. Soc.* **2007**, *129*, 7246.
(29) Anthony, J. E.; Facchetti, A.; Heeney, M.; Marder, S. R.; Zhan, X. W. *Adv. Mater.* **2010**, *22*, 3876.
(30) Zhan, X. W.; Facchetti, A.; Barlow, S.; Marks, T. J.; Ratner, M. A.; Wasielewski, M. R.; Marder, S. R. *Adv. Mater.* **2010**, DOI: 10.1002/adma.201001402.
(31) Fan, L.; Xu, Y.; Tian, H. *Tetrahedron Lett.* **2005**, *46*, 4443.
(32) Wang, H.; Wen, Y.; Yang, X.; Wang, Y.; Zhou, W.; Zhang, S.; Zhan, X.; Liu, Y.; Shuai, Z.; Zhu, D. *ACS Appl. Mater. Interfaces* **2009**, *1*, 1122.
(33) Blouin, N.; Michaud, A.; Gendron, D.; Wakim, S.; Blair, E.; Neagu-Plesu, R.; Belletete, M.; Durocher, G.; Tao, Y.; Leclerc, M. *J. Am. Chem. Soc.* **2008**, *130*, 732.
(34) Lee, B. L.; Yamamoto, T. *Macromolecules* **1999**, *32*, 1375.
(35) Huang, X. B.; Zhu, C. L.; Zhang, S. M.; Li, W. W.; Guo, Y. L.; Zhan, X. W.; Liu, Y. Q.; Bo, Z. S. *Macromolecules* **2008**, *41*, 6895.
(36) Wu, P. T.; Kim, F. S.; Champion, R. D.; Jenekhe, S. A. *Macromolecules* **2008**, *41*, 7021.
(37) Qian, G.; Dai, B.; Luo, M.; Yu, D. B.; Zhan, J.; Zhang, Z. Q.; Ma, D. G.; Wang, Z. Y. *Chem. Mater.* **2008**, *20*, 6208.

(38) Colladet, K.; Fourier, S.; Cleij, T. J.; Lutsen, L.; Gelan, J.; Vanderzande, D.; Nguyen, L. H.; Neugebauer, H.; Sariciftci, S.; Aguirre, A.; Janssen, G.; Goovaerts, E. *Macromolecules* **2007**, *40*, 65.
(39) Zhu, Z.; Waller, D.; Gaudiana, R.; Morana, M.; Muhlbacher, D.; Scharber, M.; Brabec, C. *Macromolecules* **2007**, *40*, 1981.
(40) Bayliss, N. S.; Mcrae, E. G. *J. Phys. Chem.* **1954**, *58*, 1002.
(41) Zhan, X. W.; Tan, Z.; Zhou, E.; Li, Y.; Misra, R.; Grant, A.; Domercq, B.; Zhang, X.; An, Z.; Zhang, X.; Barlow, S.; Kippelen, B.; Marder, S. R. *J. Mater. Chem.* **2009**, *19*, 5794.
(42) Wei, T. H.; Hagan, D. J.; Sense, M. J.; Van Stryland, E. W.; Perry, J. W.; Coulter, D. R. *Appl. Phys. B: Laser Opt.* **1992**, *54*, 46.
(43) Sheik-Bahae, M.; Said, A. A.; Wei, T.-H.; Hagan, D. J.; Van Stryland, E. W. *IEEE J. Quantum Electron.* **1990**, *26*, 760.